(Received 1 January 2025, Accepted 24 February 2025, Scheduled 12 March 2025)

Wideband Circularly Polarized Inverted Cup Shaped Hybrid Dielectric-Resonator Antenna over an Asymmetric Jerusalem Cross-Based Metasurface

Naresh K. Darimireddy[1], Rajasekhar Nalanagula[1,2], Runa Kumari[2], Dunya Z. Mohammed[3], Zahriladha Zakaria[4,*], and Ahmed J. A. Al-Gburi[4,*]

[1]*Department of ECE, Lendi Institute of Engineering and Technology (A), Vizianagaram, AP, India*
[2]*Department of Electrical and Electronics Engineering, BITS-Pilani, Hyderabad 500078, India*
[3]*Department of Electronic and Communications Engineering, Gilgamesh University, Baghdad, Iraq*
[4]*Center for Telecommunication Research & Innovation (CeTRI)*
Fakulti Teknologi dan Kejuruteraan Elektronik dan Komputer (FTKEK)
Universiti Teknikal Malaysia Melaka (UTeM), Durian Tunggal, Melaka 76100, Malaysia

ABSTRACT: This article introduces a Circularly-Polarized (CP) inverted cup-shaped Hybrid Cylindrical-Dielectric-Resonator-Antenna (HCDRA) combined with an asymmetric Jerusalem cross unit-cell based metasurface (MTS). The antenna, designed for use in the 5G n-79 NR band (4400–5000 MHz) and IEEE 802.11n-WLAN (5 GHz) applications, features a unique disturbed coax-feed mechanism at the edge of cylindrical DR and an asymmetric MTS that boosts the circular polarization within the DR antenna. The antenna's E-field and parametric analysis provide evidence of CP radiation. The proposed HCDRA achieves impressive S_{11} and Axial-Ratio (AR) bandwidths of 2.1 GHz and 740 MHz, with a maximum gain of 6.825 dBic. The overall gain obtained is consistently more than 5.5 dBic across the entire bandwidth of the HCDRA. The fabricated HCDRA is tested in an anechoic chamber, and the obtained practical results closely matched the simulation outcomes, confirming the performance of the proposed design.

1. INTRODUCTION

As we approach the 5G era, the n-79 band, falling under Frequency Range 1 (FR1) of sub-6 GHz frequencies, becomes increasingly important. The midpoint frequency of the 5G n-79 band is 4700 MHz, with a functional range of 4.4 to 5 GHz. There is a rising demand for wide-band, high gain integrated antennas due to their small size, light weight, and radiation efficiency [1–3]. Polarization is also crucial for antennas required in contemporary communication systems. Dielectric Resonator Antennas (DRAs) are preferred for their wide bandwidth, enhanced radiation, and low losses compared to metallic antennas. The proposed circularly polarized inverted cup-shaped HCDRA combined with an asymmetric Jerusalem cross unit-cell based metasurface is designed to meet these demands and is particularly suitable for the 5G n79 band and IEEE 802.11n WLAN applications, thereby significantly contributing to the advancement of 5G technology and the improvement of wireless communication systems.

Circularly polarized antennas are vital in various communication technologies, including Radio Frequency Identification (RFID), radar, satellite, and wireless communications. These antennas mitigate multipath fading and are better equipped to handle diverse weather conditions. Their ability to support long-distance communication makes them particularly valuable, especially as wireless networks expand. Compared to linearly polarized antennas, circularly polarized designs offer significant benefits by reducing cross-talk and enhancing mobility, making them a superior choice in many applications [4]. A comprehensive review of wideband and multiband hybrid DRAs is provided in [5], with a focus on the methods employed to achieve circular polarization (CP). One example features a proximity-coupled HDRA incorporating a hexagon-shaped split-ring slot etched to generate CP radiation [6]. Another study explores a rectangular DR antenna with perpendicular slots and a circular-ring excitation to produce wideband CP radiation [7]. CP antennas with multi-functional capability are crucial in applications like GPS, satellite, and other wireless communication systems that demand polarization concentration and resistance to multi-path fading [8]. Antennas with CP also reduce multi-path interference and simplify placement among transceiver elements. A low-profile metamaterial inspired microstrip antenna is proposed and analysed for CP radiation [9], while a 2D MTS is investigated for its ability to block and absorb electromagnetic waves [10, 11]. Planar metasurfaces have recently gained popularity for Radio Frequency (RF) and energy harvesting applications due to their advantages, such as negative permeability and refractive index properties [12, 13]. Loading MTS is a proven method for enhancing antenna bandwidth [14] and gain. Circularly polarized radiation in the DR elements can be accomplished by an offset feed

* Corresponding authors: Zahriladha Zakaria (zahriladha@utem.edu.my); Ahmed Jamal Abdullah Al-Gburi (ahmedjamal@ieee.org).

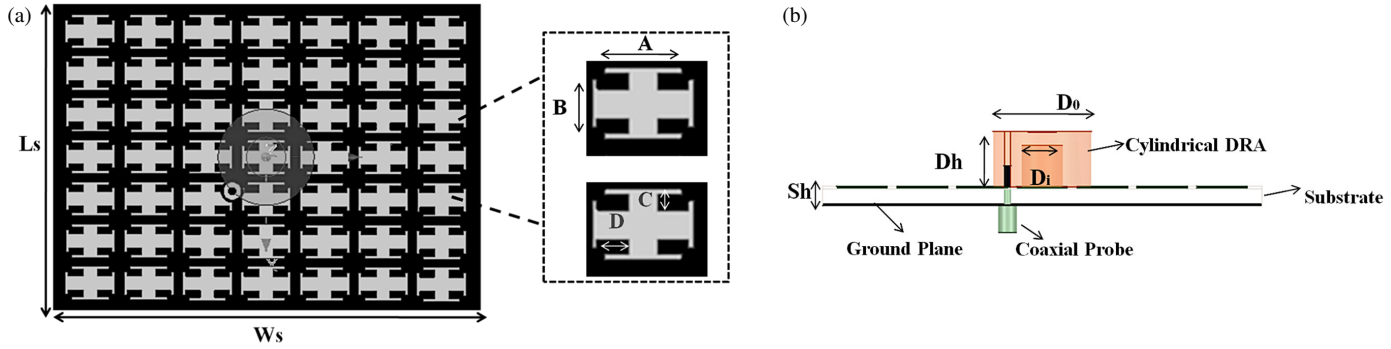

FIGURE 1. (a) Top and (b) side view of proposed HCDRA design.

and an open-ended ground slot [15] or by combining a coax-feed with a conformal E-shaped microstrip [16]. Additionally, this hybrid DRA is compared with other related standard hybrid antennas reported in prior literature [17–20]. A quasi-self-complementary MTS has been employed to create a miniaturized broadband system for circular polarization [21]. In this approach, a mushroom like MTS is paired with a DR element [22], while a rectangular DRA is loaded by MTS lens to increase the gain [23]. For dual-wideband CP radiation, a DRA loaded onto a rectangular slotted MTS has been investigated [24]. Similarly, a perturbed coax-feed at the edge of a rectangular DRA loaded onto an array of '+' shaped unicells based MTS has been utilized for wide bandwidth and CP [25].

This article presents a hybrid CDRA loaded on an altered Jerusalem cross based MTS. This design aims to achieve wide-band circularly polarized (CP) radiation with a consistent gain exceeding 5.5 dBi throughout the bandwidth. The hybrid configuration includes a cylindrical DRA, which is excited by a perturbed coax-feed and an MTS engineered to deliver broad CP radiation. The modified Jerusalem cross MTS consists of rectangular-shaped cells with varying lengths and widths. This MTS design is crucial for achieving a wide CP functional bandwidth, minimizing losses, and maintaining stable gain. The performance of proposed configuration is rigorously analysed through electromagnetic simulations using Ansys-HFSS software, ensuring the reliability and accuracy of the research findings. The fabricated HCDRA is tested and verified in an anechoic chamber, and the measured results closely match the simulation results.

2. PROPOSED HCDRA AND E-FIELD ANALYSIS

The proposed design consists of an inverted cup-shaped dielectric resonator antenna (DRA) mounted on a modified Jerusalem cross-shaped MTS, as shown in Figure 1. The hybrid cylindrical DRA (HCDRA) includes a dielectric resonator (DR) element with a height (Dh) of 10.16 mm and an outer diameter (Do) of 17 mm. The antenna is constructed using Rogers RT/Duroid 6010 (with an ε_r of 10.2 and a tan δ of 0.001) and a dielectric substrate made from Rogers RT/Duroid 5880 (thickness of 3.2 mm, ε_r of 2.2, and tan δ of 0.001). The DR element's inverted cup has a depth of 7.62 mm and an inner diameter (Di) of 7 mm. The MTS comprises an array of 7×7 modified, asymmetrical rectangular Jerusalem cross-shaped unit-cells and a ground-plane of 75 mm $\times$ 54 mm. The DRA is positioned over this MTS, with the coax-feed point located diagonally from the center of the cylindrical DR at $(-Do/2, -Do/2)$, adjusted for impedance matching to achieve wide-band CP radiation. With this asymmetric nature of feed arrangement, the DR is excited to operate in the $\text{HEM}_{11\delta}$ mode with a fundamental resonant frequency of 5 GHz. This configuration enhances the radiation performance by using the DR element as the primary radiating element and the MTS as a reflector. The combination of the DRA and MTS, as depicted in Figure 1, creates an efficient design for CP radiation, making it ideal for applications such as weather radar, global microwave data links, 5G n-79 FR1, and IEEE 802.11-n-WLAN.

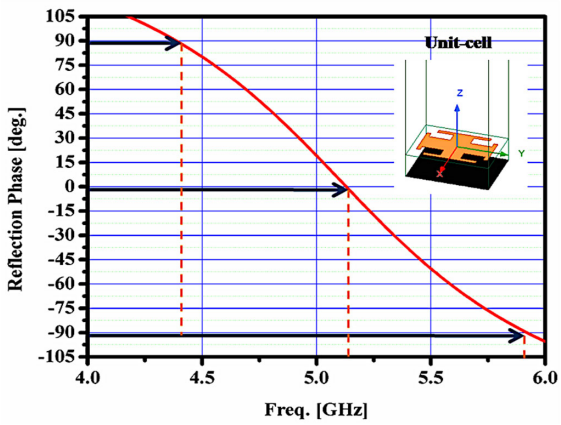

FIGURE 2. Unit-cell and reflection phase curve of unit-cell metasurface.

Figure 2 illustrates the proposed unit-cell configuration's reflection phase curve ($\pm 90°$). The reflection phase at $0°$ occurs at 5.13 GHz, with a reflection-phase ($\pm 90°$) bandwidth ranging from 4.4 GHz to 5.9 GHz, demonstrating the wide-band performance of the Jerusalem cross-shaped MTS. The unit cells of the MTS are spaced 1.4 mm apart in the normal plane and 1.6 mm in the azimuth plane. The hybrid cylindrical DRA is adjusted for broad CP radiation, with the coax-feed positioned along the diagonal for improved performance. To find the resonant hybrid ($\text{HE}_{11\delta}$) modes in hybrid cylindrical DRA, the following Equation (1) is used along with the effective permittivity and

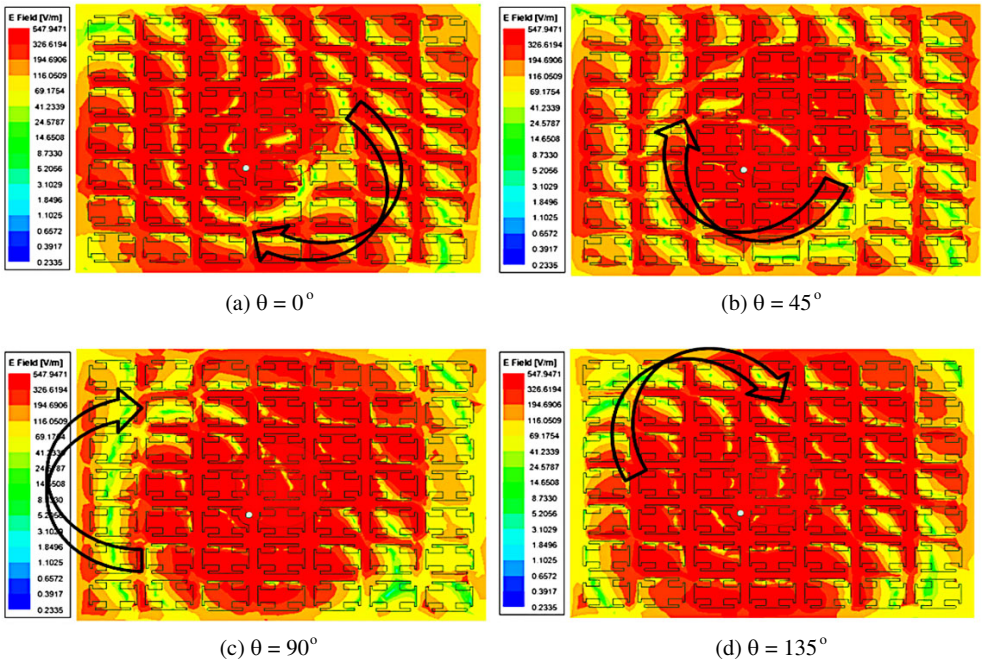

(a) θ = 0° (b) θ = 45°

(c) θ = 90° (d) θ = 135°

FIGURE 3. Magnitudes of E-field rotation on a proposed Jerusalem cross MTS at various phases.

height Equations (2) and (3).

$$f_{r,\mathrm{HE}_{11\delta}} = \frac{6.321c}{2\pi d\sqrt{\varepsilon_{r,eff}+2}}\left[0.27+0.36\,\frac{d}{2H_{eff}} +0.02\left(\frac{d}{2H_{eff}}\right)^2\right] \quad (1)$$

If a multi-segmented antenna is considered, the resonance frequency will be affected by the layers of the substrate (H_{sub}) and dielectric (H_{DR}) materials. Accordingly, the effective height (H_{eff}) and permittivity ($\varepsilon_{r,eff}$) of the hybrid CDRA are calculated by Equations (2) and (3).

$$H_{eff} = H_{\mathrm{DR}} + H_{\mathrm{sub}} \quad (2)$$

Similarly, the effective relative permittivity $\varepsilon_{r,eff}$ in Equation (4) is given by,

$$\varepsilon_{r,eff} = \frac{H_{eff}}{\frac{H_{\mathrm{DR}}}{\varepsilon_{r,\mathrm{CDRA}}} + \frac{H_{\mathrm{sub}}}{\varepsilon_{r,\mathrm{sub}}}} \quad (3)$$

where "d" ($D/2$) is the radius of the cylindrical DR element.

Figure 3 demonstrates the magnitude of the time dependent E-field ($\theta = 0$, 45, 90, and 135 degrees) of the DRA loaded MTS at 5 GHz. The circular rotation of the E-fields is manifested in the DR loaded MTS, indicating broad CP radiation. This results in the excitation of an orthogonal mode across a wide frequency range, meeting both amplitude and phase shift requirements. Additionally, Figure 3 reveals that the electric field rotates clockwise, confirming that the antenna exhibits left-hand circular polarization. To prevent performance degradation caused by the connection between coax-feed and the array of unit-cells, the metal part of the MTS of radius 2.5 mm around the feed location is etched.

3. PARAMETRIC STUDY

The performance of the proposed HCDRA is assessed through a parametric study, considering various segments of antenna designs. These include a pierced probe-fed DRA without an MTS, followed by the addition of $3*3$, $5*5$, and $7*7$ unit-cell arrays of MTS assemblies, as shown in Figure 4. The equivalent S_{11} plots for the different $N \times N$ MTS configurations are presented together in Figure 4. Introducing the MTS shifts the higher frequency range to a lower range of frequencies while maintaining CP radiation. The return loss at 5 GHz with the MTS configuration is -35 dB, and the bandwidth is 1.65 GHz, offering an increased bandwidth of 600 MHz. Additionally, the proposed MTS contributes to size reduction as the frequency shifts from higher to lower range of frequencies due to the MTS properties. Figure 5 presents S_{11} plots for various coax-feed heights, optimizing the probe height at $Ph = 5$ mm, where the enhanced bandwidth discussed earlier is achieved.

4. PROTOTYPE, ASSESSMENT AND DISCUSSION OF RESULTS

The prototype of the anticipated HCDRA, before and later the alignment, is shown in Figure 6(a). The experimental setup, illustrated in Figure 6(b), was used to measure the S_{11} using a vector network analyzer (VNA) and to assess other radiation parameters, such as axial ratio (AR), gain, and radiation pattern, to evaluate the antenna's performance. A comparison between the predicted and simulated S_{11} and AR results is provided in Figures 7 and 8, respectively. The measured results show a broad bandwidth of 2.12 GHz (from 4.38 to 6.5 GHz) and a wide 3-dB axial ratio bandwidth of 740 MHz (from 4.72 to 5.49 GHz), achieved through the use of the Jerusalem cross-

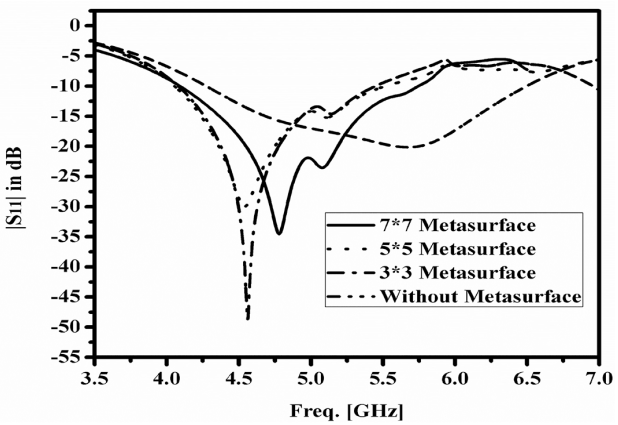

FIGURE 4. Comparison of S_{11} values for different $N \times N$ MTS designs.

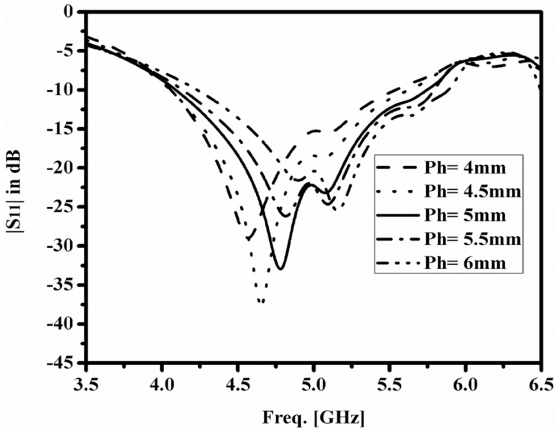

FIGURE 5. S_{11} plots for various heights of coax-feed (Ph).

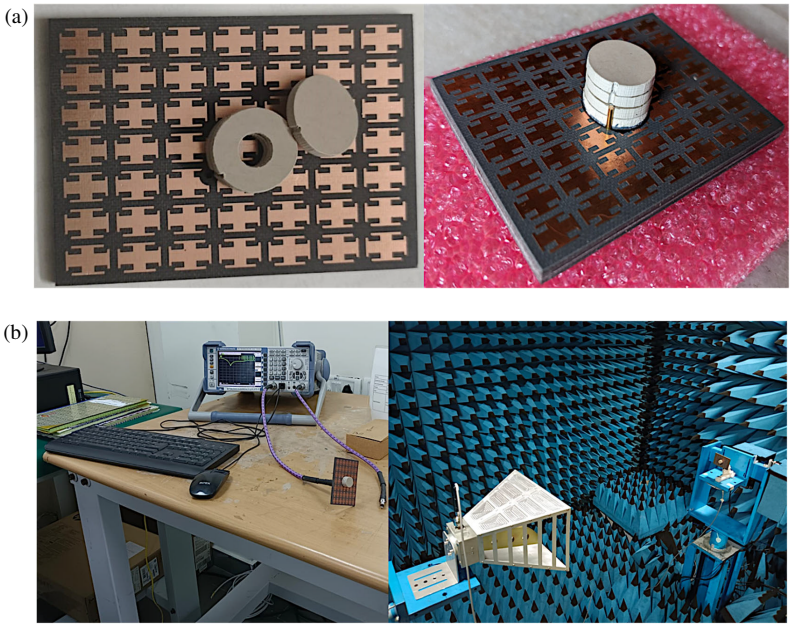

FIGURE 6. Fabricated HCDRA-2 (a) prototype before & after alignment and (b) its measurement setup in an anechoic chamber.

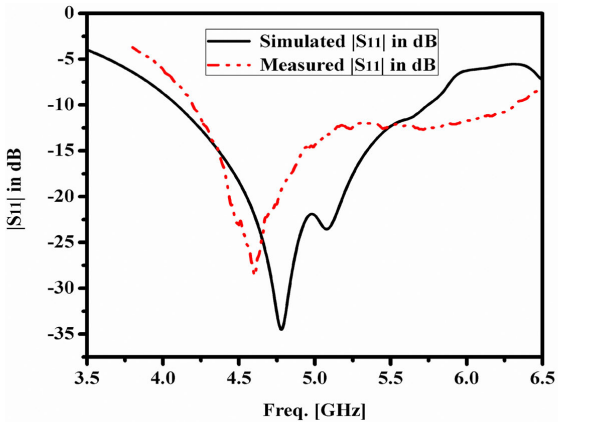

FIGURE 7. Measured vs. simulated S_{11} plots of proposed design.

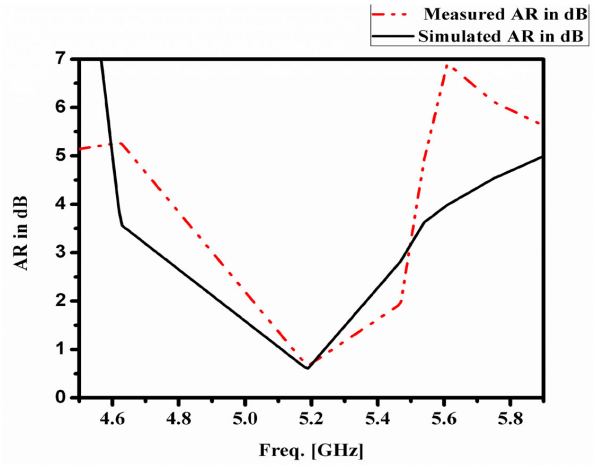

FIGURE 8. Measured vs. simulated AR plots of proposed design.

TABLE 1. Summary of measured and simulation outcomes of the proposed HCDRA.

Parameter	Simulated	Measured
Functional range of frequencies	4.097–5.747 GHz	4.19–6.32 GHz
RL-Bandwidth	1.65 GHz	2.13 GHz
AR-Bandwidth	0.59 GHz	0.74 GHz
Gain	6.72 dBic	6.852 dBic

TABLE 2. Performance assessment of the proposed with existing works reported in the open literature.

[Ref.]	Feed and DRA Structure	CP Generation Technique	Volume (λ_0^3) at resonance	RL Band-width (GHz)	Gain in dBic	Polarization conversion
[15]	Parasitically Coupled Aperture Feed & Rectangular DR	An off-set feed with a Combination of Open-ended ground-slot and Stair-shaped rectangular DR	$0.46 \times 0.46 \times 0.07$	3.844–8.146	3.9	No
[16]	A probe is combined with conformal metal strip acts as a feed and Rectangular DR	A parasitic microstrip at certain distance of conformal metal patch for the two identical rectangular shaped DR elements	$0.46 \times 0.46 \times 0.34$	3.50–4.95	6.2	No
[17]	EM Coupled	A feeding network with four microstrip lines featuring four slots arranged geometrically to ensure CP radiation	$0.8\lambda \times 0.8\lambda \times 0.12\lambda$	1.08–1.82	5	No
[18]	EM Coupled	Due to the arc-shaped slots	$0.8\lambda \times 0.8\lambda \times 0.118\lambda$	1.22–1.71	3	No
[19]	EM Coupled	Modified cross-slot	$0.43\lambda \times 0.43\lambda \times 0.29\lambda$	2.19–2.92	5	No
[20]	Dual Perpendicular Strip line	Dual vertical microstrip lines with a perpendicular L-shaped element excite orthogonal modes	$0.59\lambda \times 0.59\lambda \times 0.26\lambda$	2.82–3.83	5.5	No
[21]	Pierced Coax-feed & Cylindrical shaped DR	Quasi-self-complementary nature of the MTS	$6.08 \times 4 \times 0.06$	24.65–26.06	6.03	Yes
[24]	Pierced Coax-feed & Rectangular shaped DR	Due to the MTS and assembling of two kinds of DR elements	$0.93 \times 1.29 \times 0.16$	4.2 to 5.4 GHz and 7.62 to 8 GHz (Dual-Bands)	8.4	Yes
[25]	Disturbed coax-feed & Rectangular shaped DR	Due to "+" shaped array of unit-cells based MTS and rectangular shaped DR	$0.93 \times 1.29 \times 0.16$	3.6–6.6 GHz	6–7.2	Yes
Proposed	Perturbed Coax-feed at the edge of Cylindrical shaped DR	Optimization of feed location of DR element and asymmetric Jerusalem-cross-shaped MTS	$0.92 \times 1.25 \times 0.22$	4.19–6.32 GHz	6.852	Yes

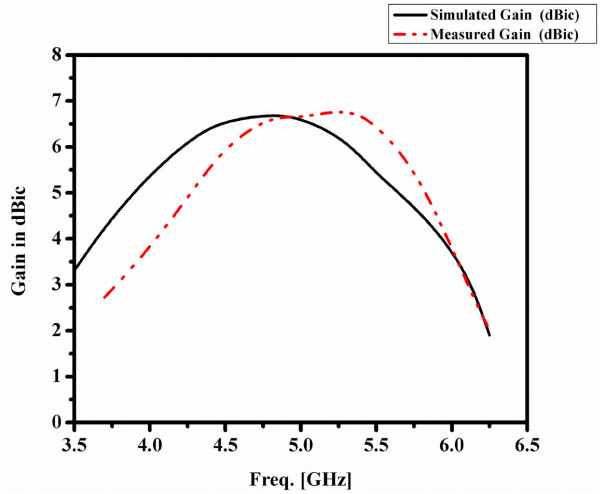

FIGURE 9. Gain vs. frequency plot.

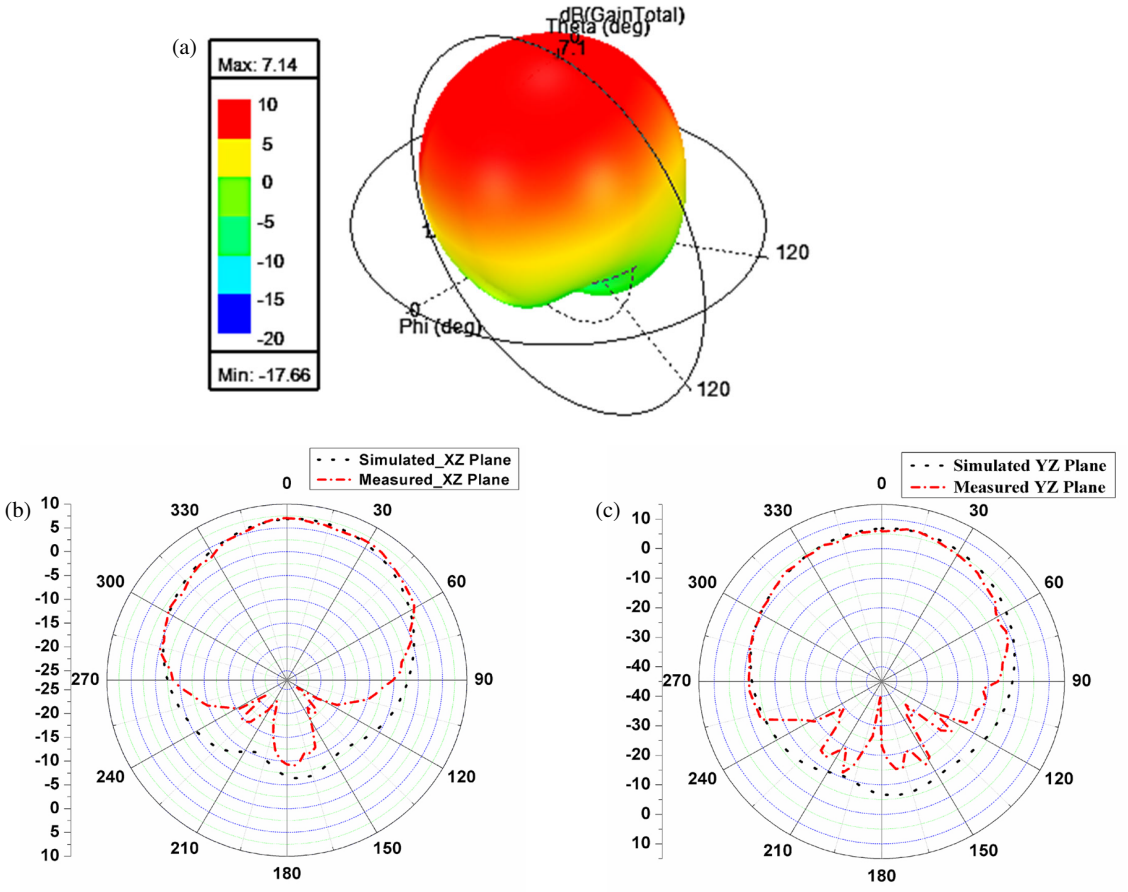

FIGURE 10. (a) 3D-gain plot. (b), (c) Measured vs. simulated radiation pattern (XZ and YZ planes) plots at 5 GHz of the proposed design.

shaped metasurface and inverted-cup-shaped DR configuration.

Figure 9 presents the gain vs. frequency plot for the proposed design, comparing simulated and measured results. The gain increases with frequency, peaking at approximately 5.5 GHz with a maximum value of around 7 dBic, before decreasing. The measured gain (red dashed line) closely aligns with the simulated gain (black solid line), demonstrating the accuracy of the design and its fabrication.

Figure 10 illustrates the measured and simulated radiation patterns of the proposed design at 5 GHz in the XZ and YZ planes. In the XZ plane, the patterns show a directional main lobe with suppressed side lobes, with reasonable agreement between the measured (red dashed line) and simulated (black dot-

ted line) results. Similarly, in the YZ plane, the patterns display a directional radiation characteristic with balanced coverage, again confirming good alignment between the measured and simulated data. These results validate the design's consistent gain performance and well-defined radiation characteristics, making it highly suitable for applications such as 5G or other advanced wireless communication systems. The slight discrepancies between measured and simulated results may be attributed to fabrication tolerances or environmental factors during testing.

It is evident from Figure 9 that the gain is consistent across the operating frequency range, i.e., above 5.5 dBi. It is also observed from Figure 10 that the measured radiation patterns in XZ and YZ planes are similar compared to the simulated patterns, and it ensures CP radiation. The measured and simulation results are briefed in Table 1, and they are in close agreement.

Compared to existing studies, the proposed design's performance is summarized in Table 2. In [15, 16], circular polarization (CP) is achieved through the feed mechanism and the arrangement of DR elements. Moreover, the proposed hybrid DRA is compared with other well-known hybrid antennas found in the literature [17–20]. The quasi-self-complementary nature of the MTS in [21] generates CP radiation, while the slotted rectangular array of unit-cells in [24] creates dual CP bands, and also '+' shaped unit-cells based hybrid DRA in [25] produces wide CP radiation. These designs operate within the frequency ranges relevant to millimeter-wave (5G-FR2) and sub 6 GHz (5G-FR1) applications. In the proposed antenna, the asymmetrical design and placement of the probe feed (related to the DR element's diameter) are key factors contributing to CP radiation. The gain of the proposed antenna remains stable across the bandwidth, outperforming other designs mentioned in Table 2.

5. CONCLUSIONS

This article introduces a cylinder-shaped hybrid DRA positioned on a Jerusalem cross-shaped metasurface to achieve broad CP radiation for 5.0 GHz wireless LAN applications. The antenna's development and configuration are presented through parametric analysis and E-field magnitude analysis, with corresponding results presented. The incorporation of the metasurface shifts the antenna's higher higher resonant frequency to a lower resonance, leading to a reduction in overall size. The design achieves an RL bandwidth of 2.13 GHz and an AR bandwidth of 740 MHz, with a maximum gain of 6.852 dBic. This proposed configuration supports CP radiation at 5 GHz, making it suitable for applications such as the 5G n-79 (FR1) band, data links, and IEEE 802.11-n-WLAN.

ACKNOWLEDGEMENT

The authors would like to thank Universiti Teknikal Malaysia Melaka (UTeM) and the Ministry of Higher Education (MOHE) of Malaysia for supporting this project.

REFERENCES

[1] Wang, C., W. Hu, X. Jiang, Q. Fan, and J. Huang, "Dual-band and dual-sense circularly polarized dielectric resonator antenna with filtering response," *Progress In Electromagnetics Research M*, Vol. 123, 127–135, 2024.

[2] Abdullah Al-Gburi, A. J., "5G MIMO antenna: Compact design at 28/38 GHz with metamaterial and SAR analysis for mobile phones," *Przegląd Elektrotechniczny*, Vol. 2024, No. 4, 171–174, 2024.

[3] Liu, H., T. Yan, S.-J. Fang, and Z. Wang, "Single-feed cylindrical dielectric resonator antenna with wide angular circular polarization," *Progress In Electromagnetics Research M*, Vol. 106, 47–57, 2021.

[4] Guo, L. and K. W. Leung, "Compact linearly and circularly polarized unidirectional dielectric resonator antennas," *IEEE Transactions on Antennas and Propagation*, Vol. 64, No. 6, 2067–2074, 2016.

[5] Nalanagula, R., N. K. Darimireddy, R. Kumari, C.-W. Park, and R. R. Reddy, "Circularly polarized hybrid dielectric resonator antennas: A brief review and perspective analysis," *Sensors*, Vol. 21, No. 12, 4100, 2021.

[6] Darimireddy, N. K. and C.-W. Park, "Electromagnetic coupled circularly polarized hybrid antenna for LTE applications," in *2020 IEEE International Symposium on Antennas and Propagation and North American Radio Science Meeting*, 401–402, Montreal, QC, Canada, 2020.

[7] Kumar, R. and R. K. Chaudhary, "Circularly polarized rectangular DRA coupled through orthogonal slot excited with microstrip circular ring feeding structure for Wi-MAX applications," *International Journal of RF and Microwave Computer-Aided Engineering*, Vol. 28, No. 1, e21153, 2018.

[8] Rajasekhar, N., R. Kumari, N. K. Darimireddy, and A. Chehri, "A hybrid dielectric resonator antenna with dual sense circular polarization for wireless LAN applications," in *Human Centred Intelligent Systems. Smart Innovation, Systems, and Technologies*, Vol. 310, 171–178, A. Zimmermann, R. J. Howlett, L. C. Jain (eds.), Springer, Singapore, 2022.

[9] Nalanagula, R., N. K. Darimireddy, R. Kumari, and C. W. Park, "Dual circularly polarized semi-cylindrical hybrid dielectric resonator antenna for X and Ku-band applications," *International Journal of RF and Microwave Computer-Aided Engineering*, Vol. 32, No. 9, e23279, 2022.

[10] Abdullah Al-Gburi, A. J., I. M. Ibrahim, K. S. Ahmad, Z. Zakaria, M. Y. Zeain, M. K. Abdulhameed, and T. Saeidi, "A miniaturised UWB FSS with stop-band characteristics for EM shielding applications," *Przegląd Elektrotechniczny*, Vol. 97, No. 8, 142–145, 2021.

[11] Sharma, A., H. Singh, A. Gupta, and A. J. A. Al-Gburi, "Development and evaluation of wideband negative response in ultra-thin polygon metamaterial," *The European Physical Journal B*, Vol. 97, No. 5, 61, 2024.

[12] Amer, A. A. G., N. Othman, S. Z. Sapuan, A. Alphones, M. F. Hassan, A. J. A. Al-Gburi, and Z. Zakaria, "Dual-band, wide-angle, and high-capture efficiency metasurface for electromagnetic energy harvesting," *Nanomaterials*, Vol. 13, No. 13, 2015, 2023.

[13] Qiu, Y., Z. Weng, Z.-Q. Zhang, J. Liu, H.-W. Yu, and Y.-X. Zhang, "A dielectric resonator fed wideband metasurface antenna with radiation pattern restoration under its high order modes," *IEEE Access*, Vol. 8, 217 671–217 680, 2020.

[14] Park, I., "Application of metasurfaces in the design of performance-enhanced low-profile antennas," *EPJ Applied*

Metamaterials, Vol. 5, 11, 2018.

[15] Lu, L., Y.-C. Jiao, H. Zhang, R. Wang, and T. Li, "Wideband circularly polarized antenna with stair-shaped dielectric resonator and open-ended slot ground," *IEEE Antennas and Wireless Propagation Letters*, Vol. 15, 1755–1758, 2016.

[16] Iqbal, J., U. Illahi, M. I. Sulaiman, M. M. Alam, M. M. Su'ud, and M. N. M. Yasin, "Mutual coupling reduction using hybrid technique in wideband circularly polarized MIMO antenna for WiMAX applications," *IEEE Access*, Vol. 7, 40 951–40 958, 2019.

[17] Massie, G., M. Caillet, M. Clenet, and Y. M. M. Antar, "A new wideband circularly polarized hybrid dielectric resonator antenna," *IEEE Antennas and Wireless Propagation Letters*, Vol. 9, 347–350, 2010.

[18] Massie, G., M. Caillet, M. Clenet, and Y. M. M. Antar, "Wideband circularly polarized hybrid dielectric resonator antenna," U.S. Patent 8,928,544, Jan. 2015.

[19] Zou, M. and J. Pan, "Wideband hybrid circularly polarised rectangular dielectric resonator antenna excited by modified cross-slot," *Electronics Letters*, Vol. 50, No. 16, 1123–1125, 2014.

[20] Chowdhury, R., N. Mishra, M. M. Sani, and R. K. Chaudhary, "Analysis of a wideband circularly polarized cylindrical dielectric resonator antenna with broadside radiation coupled with simple microstrip feeding," *IEEE Access*, Vol. 5, 19 478–19 485, 2017.

[21] Zhao, G., Y. Zhou, J. R. Wang, and M. S. Tong, "A circularly polarized dielectric resonator antenna based on quasi-self-complementary metasurface," *IEEE Transactions on Antennas and Propagation*, Vol. 70, No. 8, 7147–7151, 2022.

[22] Wang, Z., Y. Dong, Z. Peng, and W. Hong, "Hybrid metasurface, dielectric resonator, low-cost, wide-angle beam-scanning antenna for 5G base station application," *IEEE Transactions on Antennas and Propagation*, Vol. 70, No. 9, 7646–7658, 2022.

[23] George, E. and C. Saha, "Metasurface lens-integrated rectangular dielectric resonator antenna with enhanced gain," *Journal of Electronic Materials*, Vol. 51, No. 6, 3059–3067, 2022.

[24] Kiyani, A., M. Asadnia, S. M. Abbas, K. P. Esselle, and A. Mahmoud, "Wide dual-band circularly polarized diecletric resonator: Innovative integration of a single hybrid feed and thin grounded metasurface," *Micromachines*, Vol. 14, No. 7, 1432, 2023.

[25] Kiyani, A., N. Nasimuddin, R. M. Hashmi, A. A. Baba, S. M. Abbas, K. P. Esselle, and A. Mahmoud, "A single-feed wideband circularly polarized dielectric resonator antenna using hybrid technique with a thin metasurface," *IEEE Access*, Vol. 10, 90 244–90 253, 2022.